InPrime: Indonesian Journal of Pure and Applied Mathematics
Vol. 8, No. 1 (2026), pp. 40 – 55, doi: 10.15408/inprime.v8i1.49631
p-ISSN 2686-5335, e-ISSN: 2716-2478

# Optimal Control Analysis of a Human-Animal Nipah Virus Transmission Model

Ratna Widayati*, Ramya Rachmawati, Yulian Fauzi, Septri Damayanti, and Arlin Marsyanda
Department of Mathematics, Faculty of Mathematics and Natural Sciences, Universitas Bengkulu, Bengkulu, Indonesia
Email:*rwidayati@unib.ac.id

## Abstract

This study proposes a novel multi-host SIRS optimal control model for Nipah virus transmission involving bats, pigs, and humans, extending classical SIR/SEIR frameworks by explicitly incorporating cross-species transmission, reinfection, and heterogeneous contact pathways supported by ecological evidence. Unlike uncontrolled epidemic models, the proposed framework integrates three time-dependent interventions: infected-pig culling, human–animal protective measures, and isolation of infected humans, allowing simultaneous evaluation of epidemiological impact and implementation cost. The existence of an optimal control set is established, and Pontryagin's Maximum Principle is applied to derive the necessary optimality system. Numerical simulations show that coordinated interventions substantially outperform no-control scenarios. The peak number of infected humans decreases from more than 650,000 to approximately 70,000, while the peak number of infected pigs declines from over 68,000 to about 16,000. Control trajectories indicate that strong early implementation of all measures is the most effective strategy, followed by gradual relaxation as prevalence declines, leading to more efficient resource allocation over time. Compared with classical single-host SIR/SEIR models, the proposed model better captures interspecies spillover dynamics and enables evaluation of integrated response policies that cannot be represented in simpler frameworks. These findings demonstrate the importance of coordinated multi-component strategies for mitigating Nipah outbreaks across interacting host populations. A limitation of this study is the use of assumed parameter values in several transmission processes; future work may incorporate data-driven calibration, stochastic effects, spatial mobility, and uncertainty analysis to improve predictive accuracy.
**Keywords:** Interspecies transmission; Nipah virus; Optimal control; Population dynamics; SIRS model.

## Abstrak

*Penelitian ini mengusulkan model optimal kontrol SIRS multi-host yang baru untuk penularan virus Nipah yang melibatkan kelelawar, babi, dan manusia, sebagai pengembangan dari kerangka klasik SIR/SEIR dengan secara eksplisit memasukkan penularan antarspesies, reinfeksi, serta jalur kontak heterogen yang didukung oleh bukti ekologis. Berbeda dengan model epidemi tanpa kontrol, kerangka yang diusulkan mengintegrasikan tiga intervensi bergantung waktu, yaitu pemusnahan babi terinfeksi, tindakan perlindungan manusia–hewan, dan isolasi manusia terinfeksi, sehingga memungkinkan evaluasi simultan terhadap dampak epidemiologis dan biaya implementasi. Keberadaan himpunan kontrol optimal dibuktikan, dan Prinsip Maksimum Pontryagin diterapkan untuk menurunkan sistem syarat optimalitas yang diperlukan. Simulasi numerik menunjukkan bahwa intervensi terkoordinasi secara signifikan lebih unggul dibandingkan skenario tanpa kontrol. Puncak jumlah manusia terinfeksi menurun dari lebih dari 650.000 menjadi sekitar 70.000, sedangkan puncak babi terinfeksi turun dari lebih dari 68.000 menjadi sekitar 16.000. Profil kontrol menunjukkan bahwa penerapan kuat pada tahap awal untuk seluruh tindakan merupakan strategi paling efektif, kemudian dikurangi secara bertahap seiring menurunnya prevalensi sehingga menghasilkan alokasi sumber daya yang lebih efisien dari waktu ke waktu. Dibandingkan model klasik SIR/SEIR satu-host, model yang diusulkan lebih mampu menggambarkan dinamika spillover antarspesies serta mengevaluasi kebijakan respons terpadu yang tidak dapat direpresentasikan pada model yang lebih sederhana. Temuan ini menegaskan pentingnya strategi multi-komponen yang terkoordinasi dalam mitigasi wabah Nipah pada populasi host yang saling berinteraksi. Keterbatasan penelitian ini adalah penggunaan beberapa nilai parameter asumsi pada proses transmisi tertentu; penelitian selanjutnya dapat*

*) Corresponding author
Submitted December 14th, 2025, Revised May 14th, 2026,
Accepted for publication May 24th, 2026, Published Online May 31st, 2026

*memasukkan kalibrasi berbasis data, efek stokastik, mobilitas spasial, dan analisis ketidakpastian untuk meningkatkan akurasi prediksi.*
***Kata Kunci:*** *Penularan antarspesies; Nipah virus; Kontrol optimal; Dinamika populasi; Model SIRS.*

**2020MSC:** 49J15

## 1. INTRODUCTION

Zoonosis is an infectious disease transmitted from animals to humans as a result of infection in animal hosts. These diseases may arise from bacterial, viral, parasitic, or atypical pathogens and can be transmitted through direct contact, consumption of contaminated food or water, or exposure to a polluted environment. Because of the close interconnection between humans, animals, and the natural ecosystem, zoonotic pathogens pose a serious global public health challenge [1]. The Nipah virus (NiV) is one of the most recently identified zoonotic pathogens, originating from the Paramyxoviridae family. It represents an emerging infectious agent capable of crossing species barriers, with fruit bats of the genus Pteropus recognized as its primary natural reservoir. NiV has been classified by the World Health Organization (WHO) as a priority pathogen under its R&D Blueprint, owing to its high virulence, potential for human-to-human transmission, complex zoonotic behavior, and the current lack of effective treatment or preventive measures [2].

NiV can be transmitted between humans through unhygienic contact with the body of an infected person, particularly during funeral or burial practices [3]. The initial outbreak in Malaysia was associated with pigs that harbored and transmitted the virus to pig farmers, leading to widespread infections [2]. According to [4], fruit bats of the Pteropus genus, belonging to the Pteropodidae family, serve as the primary natural reservoir of NiV. These bats are believed to have transmitted the virus to pigs through saliva, urine, or partially eaten fruits contaminated with the pathogen. Once pigs became infected, they acted as amplifying hosts, facilitating the transmission of the virus to humans and triggering the Malaysian epidemic. Henipaviruses, members of the Paramyxoviridae family, exhibit sustained circulation within bat colonies through frequent bat-to-bat transmission, which enables their endemic persistence and occasional spillover to other animal hosts and humans [5]. Furthermore, experimental and field evidence indicate that the Nipah virus can spread efficiently among swine within affected farms, likely via respiratory and oropharyngeal secretions from infected animals [6].

In September 1998, an outbreak of acute febrile encephalitis with considerable mortality occurred among individuals involved in pig farming in Peninsular Malaysia. The etiological agent, later designated as the Nipah virus, was confirmed in March 1999 following its isolation from the cerebrospinal fluid of an infected patient in Sungai Nipah village, from which the virus derived its name [7]. By mid-June 1999, Malaysia had reported over 265 cases of encephalitis resulting in 105 deaths, while Singapore documented 11 cases of encephalitis or respiratory illness, including one fatality [8], [9]. Following the initial detection of NiV in Bangladesh in 2001, sporadic outbreaks were reported in areas near West Bengal, a state in India adjacent to Bangladesh. However, in May 2018, a sudden epidemic occurred in Kerala, a southern Indian state far from the Bangladesh border, followed by another outbreak in the subsequent season [10], [11]. According to the World Health Organization (WHO), several countries, including Cambodia, Ghana, Indonesia, Madagascar, the Philippines, and Thailand, are considered at risk of Nipah virus infection. Indonesia, in particular, is classified as high-risk due to its tropical climate and rich biodiversity, which provide favorable ecological conditions for fruit bats, the natural reservoirs of the virus [12].

NiV has spread across multiple regions, resulting in significant health and economic impacts. Therefore, understanding its transmission dynamics is crucial, and various studies have investigated its zoonotic spread, human transmission routes, and outbreak modeling, including the works of [13] developed a NiV transmission model with optimal control applied solely to the human population, using awareness, treatment, and quarantine as control variables aimed at minimizing the number of infected individuals. The study in [14] proposed an SEIR model focused exclusively on the human population to analyze the local and global stability of the NiV transmission dynamics without incorporating control measures. Meanwhile, the study in [15] developed an SIRN model with optimal control applied to the human population, utilizing two control variables, enhancing public awareness and improving healthcare interventions. [16] developed a human-based SIRD model and conducted three-dimensional simulations to examine the transmission behavior of the Nipah virus. In contrast, the authors in [17] formulated a three-population SEIR model involving humans, pigs, and bats without incorporating optimal control analysis, while the research in [18] proposed an SIRN model with awareness and treatment as control variables, and the author [19] investigated a human SIRD model featuring a specific transmission rate but no control parameters. Reference [20] proposed an SEIRT model focusing on the human population using real data from Bangladesh without incorporating control variables, whereas Muhammad Younas Khan developed an SVITR model involving humans and flying foxes with optimal control strategies. Similarly, the authors [21] formulated an SEIVR model for human and animal populations in general, without distinguishing between bats and pigs, while the study in [2] analyzed an SVIRD model that explicitly separated bats and pigs within two populations and applied optimal control to examine the disease dynamics. Reference [7] examined an SIR model for NiV transmission involving three species: humans, pigs, and bats, conducting both local and global stability analyses without incorporating control variables, while the authors [1] developed a similar three-species model in which the bat population was divided into only two compartments (S and I) and performed an optimal control analysis.

This study extends previous Nipah virus models by proposing a novel multi-host SIRS framework involving humans, bats, and pigs. Unlike earlier studies, the model incorporates reinfection dynamics, direct and indirect interspecies transmission, and three time-dependent control strategies: protective measures, infected-pig culling, and isolation of infected humans. From a mathematical perspective, the SIRS structure enables the analysis of recurring outbreaks and long-term disease persistence. The main objective of this study is to determine an optimal control strategy that minimizes the number of infected pigs and humans while reducing intervention costs.

## 2. METHOD

The proposed model considers three interacting populations: bats, pigs, and humans. Each population is divided into three epidemiological compartments, namely susceptible, infected, and recovered, so that the overall system consists of three interconnected SIRS sub-models. Recovered individuals are assumed to lose immunity over time and return to the susceptible class.

The model is constructed under the following assumptions: (i) bats act as the natural reservoir of Nipah virus and can transmit infection to bats, pigs, and humans; (ii) pigs function as intermediate hosts and can transmit infection to pigs and humans; (iii) humans can transmit infection only to other humans; (iv) transmission from humans to bats or pigs, and from pigs to bats, is neglected due to its very low likelihood; (v) each population experiences recruitment and natural mortality; and (vi) all individuals within the same population mix homogeneously. Based on these assumptions, the

transmission pathways considered are bat-to-bat, bat-to-pig, bat-to-human, pig-to-pig, pig-to-human, and human-to-human transmission (see Figure 1).

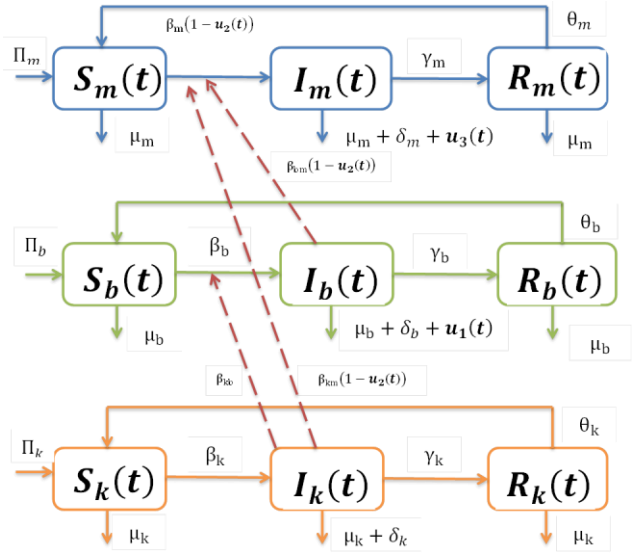


**Figure 1.** The dynamic flowchart of the model

The overall human population $N_m(t)$ at a given time $t$ is categorized into three groups: susceptible humans $S_m(t)$, infected humans $I_m(t)$ and recovered humans $R_m(t)$. Thus,

$$N_m(t) = S_m(t) + I_m(t) + R_m(t).$$

The total pig population $N_b(t)$ (as the intermediate host) and the total bat population $N_k(t)$ (as the reservoir host) at time $t$ are each divided into three compartments: susceptible $(S_b(t), S_k(t))$, infected $(I_b(t), I_k(t))$ and recovered $(R_b(t), R_k(t))$ individuals, respectively. For convenience, the time-dependent notation will be simplified in the subsequent analysis. Accordingly, the variables will be written as $S_m, I_m, R_m, S_b, I_b, R_b, S_k, I_k, R_k$ instead of $S_m(t), I_m(t), R_m(t), S_b, (t), I_b(t), R_b(t), S_k(t), I_k(t), R_k(t)$, respectively, without altering their meaning. For a complete specification of the parameters, along with their descriptions, see Table 1.

Furthermore, a control set $U = \{u_1(t), u_2(t), u_3(t)\}$ is introduced. The control $u_1(t)$ denotes the culling rate of the infected pig population at time $t$. Human individuals are required to take necessary precautions when interacting with infected persons, working on animal farms, or collecting date palm sap. The control $u_2(t)$ represents the preventive effort to ensure safe interactions among humans, and between humans and infected pigs or bats, through the use of protective materials at the time $t$. The third control $u_3(t)$ denotes the effort devoted to the isolation of infected human individuals at the time $t$. For simplicity of notation, the time dependence of the control variables will be omitted in the subsequent analysis. Hence, the controls will be denoted $(u_1, u_2, u_3)$ instead of $(u_1(t), u_2(t), u_3(t))$, without any loss of generality or change in meaning.

**Table 1**. Description of parameters used in the model

| Parameters | Description |
|---|---|
| $\Pi_m$ | The human birth rate |
| $\Pi_b$ | The pig birth rate |
| $\Pi_k$ | The bat birth rate |
| $\mu_m$ | The human death rate |
| $\mu_b$ | The pig death rate |
| $\mu_k$ | The bat death rate |
| $\delta_m$ | Disease-induced mortality rate in humans |
| $\delta_b$ | Disease-induced mortality rate in pigs |
| $\delta_k$ | Disease-induced mortality rate in bats |
| $\gamma_m$ | Recovery rate for humans |
| $\gamma_b$ | Recovery rate for pigs |
| $\gamma_k$ | Recovery rate for bats |
| $\theta_m$ | Immunity loss rate of recovered humans |
| $\theta_b$ | Immunity loss rate of recovered pigs |
| $\theta_k$ | Immunity loss rate of recovered bats |
| $\beta_m$ | Rates of transmission among humans |
| $\beta_b$ | Rates of transmission among pigs |
| $\beta_k$ | Rates of transmission among bats |
| $\beta_{bm}$ | Pig to human transmission rate |
| $\beta_{km}$ | Bat to human transmission rate |
| $\beta_{kb}$ | Bat to pig transmission rate |

The optimal control system is presented as follows.

$$\dot{S}_m = \Pi_m + \theta_m R_m - \mu_m S_m - (1-u_2)(\beta_m S_m I_m + \beta_{bm} S_m I_b + \beta_{km} S_m I_k), \tag{1a}$$
$$\dot{I}_m = (1-u_2)(\beta_m S_m I_m + \beta_{bm} S_m I_b + \beta_{km} S_m I_k) - (\gamma_m + \mu_m + \delta_m + u_3) I_m, \tag{1b}$$
$$\dot{R}_m = \gamma_m I_m - (\mu_m + \theta_m) R_m, \tag{1c}$$
$$\dot{S}_b = \Pi_b + \theta_b R_b - \mu_b S_b - (\beta_b S_b I_b + \beta_{kb} S_b I_k), \tag{1d}$$
$$\dot{I}_b = (\beta_b S_b I_b + \beta_{kb} S_b I_k) - (\gamma_b + \mu_b + \delta_b + u_1) I_b, \tag{1e}$$
$$\dot{R}_b = \gamma_b I_b - (\mu_b + \theta_b) R_b, \tag{1f}$$
$$\dot{S}_k = \Pi_k + \theta_k R_k - \mu_k S_k - \beta_k S_k I_k, \tag{1g}$$
$$\dot{I}_k = \beta_k S_k I_k - (\mu_k + \delta_k + \gamma_k) I_k, \tag{1h}$$
$$\dot{R}_k = \gamma_k I_k - (\mu_k + \theta_k) R_k, \tag{1i}$$

with nonnegative initial conditions.

## 3. RESULTS

Our objective is to minimize the overall number of infected pigs and infected human individuals, as well as the costs associated with implementing the three control measures $u_1, u_2, u_3$, over the time interval $[0, t_{max}]$. The objective function is defined as follows:

$$J(u_1, u_2, u_3) = \int_0^{t_{max}} \left( c_1 I_m + c_2 I_b + \frac{1}{2}(d_1 {u_1}^2 + d_2 {u_2}^2 + d_3 {u_3}^2) \right) dt.$$

In the above equation, the terms $c_1 I_m$ and $c_2 I_b$ represent the costs associated with infected pigs and infected human individuals, respectively, where $c_1, c_2 > 0$, and are to be minimized. The subsequent three terms denote the systematic costs of the control measures, characterized by positive weighting parameters $d_1, d_2$ and $d_3$, which serve to balance the magnitudes of the control variables.

### 3.1. Existence of Optimal Control

We investigate the presence of an optimal control for the proposed problem using the theoretical framework established by Fleming and Rishel [22].

**Theorem 1.** Let the control set $U$ be defined as

$$U = \{u = (u_1, u_2, u_3) \in L^{\infty}([0, t_{max}]; \mathbb{R}^3) : 0 \leq u_i(t) \leq 1, \text{a. e. on } [0, t_{max}], i = 1,2,3\}.$$

Consider the objective functional

$$J(u_1, u_2, u_3) = \int_0^{t_{max}} \left( c_1 I_m + c_2 I_b + \frac{1}{2}(d_1 {u_1}^2 + d_2 {u_2}^2 + d_3 {u_3}^2) \right) dt.$$

Assume that:

1. The state system can be written as

$$\dot{x}(t) = f\big(t, x(t), u(t)\big), \text{ with } x(0) = x_0,$$

   where $f$ is continuous in all variables, measurable in $t$, and locally Lipschitz continuous with respect to $x$.
2. There exist constants $C_1, C_2 > 0$ such that

$$\|f(t, x, u)\| \leq C_1(1 + \|x\|) + C_2\|u\|.$$

3. The control set $U$ is nonempty, convex and closed in $L^{\infty}([0, t_{max}])$
4. The integrand of the objective functional is convex in $u$.
5. There exist constants $A, B > 0$ such that

$$K(t, x, u) \geq A\|u\|^2 - B.$$

Then there exists an optimal control triplet $u^* = ({u_1}^*, {u_2}^*, {u_3}^*)$ such that

$$J(u^*) = \min_{u \in U} J(u).$$

**Proof.**
Let the system dynamics be expressed as

$$\dot{x} = f(t, x, u), \quad x(0) = x_0,$$

where $x(t)$ represents the vector of state variables $(S_m, I_m, R_m, S_b, I_b, R_b, S_k, I_k, R_k)$ and $u(t) = \big(u_1(t), u_2(t), u_3(t)\big)$ belongs to the admissible control set is defined by

$$U = \{u = (u_1, u_2, u_3) \in L^\infty([0, t_{max}]; \mathbb{R}^3) : 0 \le u_i(t) \le 1, \text{a. e. on } [0, t_{max}], i = 1,2,3\}.$$

The objective functional is given by

$$J(u_1, u_2, u_3) = \int_0^{t_{max}} \left( c_1 I_m + c_2 I_b + \frac{1}{2}(d_1 {u_1}^2 + d_2 {u_2}^2 + d_3 {u_3}^2) \right) dt.$$

We verify the standard conditions for the existence of an optimal control.

(i). Nonemptiness of the admissible set
The set $U$ is nonempty since the zero control $u(t) = (0,0,0)$ belongs to $U$. For every $u \in U$ the right-hand side $f(t, x, u)$ is continuous in $x$ and measurable in $t$ and locally Lipschitz continuous with respect to $x$, since each component of the model consists of polynomial and bilinear terms. Hence, by the classical Carathéodory existence theorem for ordinary differential equations, the state system admits a unique solution on $[0, t_{max}]$. Therefore, the set of admissible control state pairs is nonempty.

(ii). Boundedness and positivity of the state variables
Adding the corresponding equations for each population group gives

$$\dot{N}_m = \Pi_m - \mu_m N_m - (\delta_m + u_3) I_m \le \Pi_m - \mu_m N_m,$$

and analogously for $N_b$ and $N_k$. By the differential inequality,

$$0 < N_m \le \frac{\Pi_m}{\mu_m}, \quad 0 < N_b \le \frac{\Pi_b}{\mu_b}, \quad 0 < N_k \le \frac{\Pi_k}{\mu_k},$$

tor all $t \ge 0$. Consequently, all state variables remain nonnegative and uniformly bounded. Hence, the trajectories evolve in a compact positively invariant region.

(iii). Linear growth of the system
Since the control variables appear linearly in the state equations, there exist positive constants $C_1$ and $C_2$ such that

$$\|f(t, x, u)\| \le C_1(1 + \|x\|) + C_2\|u\|.$$

for all admissible $(t, x, u)$. Thus, the state system satisfies the standard linear growth condition.

(iv). Convexity and closedness of the control set
The set $U$ is defined by the pointwise constraints $0 \le u_i \le 1$, for $i = 1,2,3$.
Hence, $U$ is convex. Moreover, it is closed in $L^2([0, t_{max}]: \mathbb{R}^3)$, and therefore weakly closed.

(v). Convexity and coercivity of the integrand
The integrand of the objective functional is

$$K(t, x, u) = c_1 I_m + c_2 I_b + \frac{1}{2}(d_1 {u_1}^2 + d_2 {u_2}^2 + d_3 {u_3}^2).$$

For each fixed $(t, x)$ the function $K$ is convex in $u$, since the quadratic terms satisfy $d_i > 0$. Furthermore, letting

$$A = \frac{1}{2}\min\{d_1, d_2, d_3\} > 0,$$

there exists $B > 0$ such that

$$K(t,x,u) \geq A\|u\|^2 - B.$$

Hence, the functional $J(u)$ is coercive and bounded from below.

(vi). Existence of a minimizing control

Let $\{u^n\} \subset U$ be a minimizing sequence such that

$$J(u^n) \to \inf_{u\in U} J(u) = m.$$

By coercivity, $\{u^n\}$ is bounded in $L^2([0,t_{max}];\mathbb{R}^3)$. Since $L^2$ is reflexive, there exists a subsequence, still denoted by $\{u^n\}$, and a function $u^* \in U$ such that $u^n \to u^*$ weakly in $L^2$.

The corresponding state solutions $\{x^n\}$ are uniformly bounded and equicontinuous. By the Arzelà–Ascoli theorem, a subsequence converges uniformly to a trajectory $x^*$, which satisfies the state system associated with $u^*$. Since $K(t,x,u)$ is convex in $u$, the functional $J(u)$ is weakly lower semicontinuous. Therefore,

$$J(u^*) \leq \lim_{n\to\infty} \inf J(u^n) = m.$$

Thus, $u^*$ attains the minimum of $J$.

Hence, there exists an optimal control triplet

$$u^* = ({u_1}^*, {u_2}^*, {u_3}^*) \in U$$

such that

$$J({u_1}^*, {u_2}^*, {u_3}^*) = \min_{(u_1,u_2,u_3)\in U} J(u_1,u_2,u_3).$$

This completes the proof. ■

### 3.2. Characterization of Optimal Control

An optimal control exists that maximizes the objective functional $J(u_1,u_2,u_3)$ subject to the aforementioned state system equations. The necessary conditions for this optimal control are derived using Pontryagin's Maximum Principle. We examine the characterization of the optimal control corresponding to $J(U)$ and the state system. This characterization is obtained from the Hamiltonian function $H$, is defined as follows:

$$H(t,x,u,\lambda) = K(t,x,u) + \sum_{i=1}^{9} \lambda_i f_i(x,u), \tag{2}$$

where $K(t,x,u)$ is an integrand of an objective functional $J$ and $f_i(x,u)$ are the right-hand sides of the $i$-th equation in the state system (1).

**Theorem 2.** Let $u^* = ({u_1}^*, {u_2}^*, {u_3}^*)$ be an optimal control in the control space $U$, along with the solution $X^* = ({S_m}^*, {I_m}^*, {R_m}^*, {S_b}^*, {I_b}^*, {R_b}^*, {S_k}^*, {I_k}^*, {R_k}^*)$ for the associated state system $X$. Then, there exist adjoint variables $\lambda_i(t), i = 1,2,3,\ldots 9$, such that the Hamiltonian function is defined by

$$H(t,x,u,\lambda) = K(t,x,u) + \sum_{i=1}^{9} \lambda_i f_i(x,u),$$

where $K(t,x,u)$ is an integrand of the objective functional $J$ and $f_i(x,u)$ are the right-hand sides of the $i$-th equation in the state system (1). The adjoint variables satisfy $\dot{\lambda}_i = -\frac{\partial H}{\partial x_i},\ i = 1,2,3,\dots,9$, with transversality conditions $\lambda_i(t_{max}) = 0,\ i = 1,2,3,\dots,9$. Furthermore, the optimal controls are characterized by the stationary conditions $\frac{\partial H}{\partial u_j} = 0,\ j = 1,2,3$. Hence, $u_1 = \frac{\lambda_5 I_b}{d_1},\ u_2 = \frac{(\lambda_2-\lambda_1)F_m}{d_2},$ $u_3 = \frac{\lambda_2 I_m}{d_3}$. Since $0 \le u_j \le 1$, the optimal controls are obtained by projection onto the admissible control set $[0,1]$:

$$\begin{cases} {u_1}^* = min\left\{1, max\left\{0, \frac{\lambda_5 {I_b}^*}{d_1}\right\}\right\} \\ {u_2}^* = min\left\{1, max\left\{0, \frac{(\lambda_2-\lambda_1)F_m}{d_2}\right\}\right\} \\ {u_3}^* = min\left\{1, max\left\{0, \frac{\lambda_2 {I_m}^*}{d_3}\right\}\right\}, \end{cases}$$

where $F_m = \beta_m {S_m}^* {I_m}^* + \beta_{bm} {S_m}^* {I_b}^* + \beta_{km} {S_m}^* {I_k}^*$.

**Proof.**
According to Pontryagin's Maximum Principle, differentiating the Hamiltonian leads to the formulation of the adjoint system, which can be expressed as follows:

$$\dot{\lambda}_1 = -\frac{\partial H}{S_m} = \lambda_1\big(\mu_m + (1-u_2)(\beta_m I_m + \beta_{bm} I_b + \beta_{km} I_k)\big) - \lambda_2\big((1-u_2)(\beta_m I_m + \beta_{bm} I_b + \beta_{km} I_k)\big),$$
$$\dot{\lambda}_2 = -\frac{\partial H}{I_m} = -c_1 + \lambda_1\Big(\big(1-u_2(t)\big)(\beta_m S_m)\Big) + \lambda_2\big(-(1-u_2)\beta_m S_m + (\gamma_m \mu_m + \delta_m + u_3)\big) - \lambda_3 \gamma_m,$$
$$\dot{\lambda}_3 = -\frac{\partial H}{R_m} = -\lambda_1 \theta_m + \lambda_3(\mu_m + \theta_m),$$
$$\dot{\lambda}_4 = -\frac{\partial H}{S_b} = \lambda_4(\mu_b + \beta_b I_b + \beta_{kb} I_k) - \lambda_5(\beta_b I_b + \beta_{kb} I_k),$$
$$\dot{\lambda}_5 = -\frac{\partial H}{I_b} = -c_2 - \lambda_1\Big(\big(1-u_2(t)\big)\beta_{bm} S_m\Big) + \lambda_4(\beta_b S_b) + \lambda_5(\gamma_b + \mu_b + \delta_b + u_1 - \beta_b S_b) - \lambda_6 \gamma_b,$$
$$\dot{\lambda}_6 = -\frac{\partial H}{R_b} = -\lambda_4 \theta_b + \lambda_6(\mu_b + \theta_b),$$
$$\dot{\lambda}_7 = -\frac{\partial H}{S_k} = \lambda_7(\mu_k + \beta_k I_k) - \lambda_8 \beta_k I_k,$$
$$\dot{\lambda}_8 = -\frac{\partial H}{I_k} = -\lambda_1(1-u_2)\beta_{km} S_m + \lambda_7 \beta_k S_k + \lambda_8(\mu_k + \delta_k + \gamma_k - \beta_{kb} S_b) - \lambda_9 \gamma_k,$$
$$\dot{\lambda}_9 = -\frac{\partial H}{R_k} = -\lambda_7 \theta_k + \lambda_9(\mu_k + \theta_k),$$

with transversality conditions $\lambda_i(t_{max})$ for $i = 1,2,3,\dots,9$. The control set $u^* = ({u_1}^*, {u_2}^*, {u_3}^*)$ satisfies the necessary condition $\frac{\partial H}{\partial u_1} = \frac{\partial H}{\partial u_2} = \frac{\partial H}{\partial u_3} = 0$. Hence, the optimal control triplet $({u_1}^*, {u_2}^*, {u_3}^*)$ is given by ${u_1}^* = \frac{\lambda_5 {I_b}^*}{d_1},\quad {u_2}^* = \frac{(\lambda_2-\lambda_1)F_m}{d_2}$ where $F_m = \beta_m {S_m}^* {I_m}^* + \beta_{bm} {S_m}^* {I_b}^* + \beta_{km} {S_m}^* {I_k}^*$, and ${u_3}^* = \frac{\lambda_2 {I_m}^*}{d_3}$.

Using standard optimal control approaches and considering the constraints on the control variables, the optimal control expressions can be easily derived. The derivation follows the usual control theory procedures and respects the admissible bounds, as shown below

$$u_1^* = min\left\{1, max\left\{0, \frac{\lambda_5 I_b^*}{d_1}\right\}\right\}$$
$$u_2^* = min\left\{1, max\left\{0, \frac{(\lambda_2 - \lambda_1)F_m}{d_2}\right\}\right\}$$
$$u_3^* = min\left\{1, max\left\{0, \frac{\lambda_2 I_m^*}{d_3}\right\}\right\}.$$

Hence, $(u_1^*, u_2^*, u_3^*)$ constitutes the optimal control that satisfies the necessary conditions for optimality. ■

### 3.3. Numerical Simulation

The analysis is subsequently extended to the optimal control system, with the forward backward sweep method implemented in Python to solve the corresponding optimality system. In the simulations, the assumptions $c_1 = c_2 = d_1 = d_2 = d_3 = 1$ are applied. All parameters are expressed in units of day$^{-1}$, as presented in Table 2.

**Table 2**. Value of parameters

| Parameters | Description | Value | Source |
|---|---|---|---|
| $\Pi_m$ | The human birth rate | 6.69852 | [7] |
| $\Pi_b$ | The pig birth rate | 0.411 | [7] |
| $\Pi_k$ | The bat birth rate | 300.3 | [7] |
| $\mu_m$ | The human death rate | 0.0000379 | [7] |
| $\mu_b$ | The pig death rate | 0.00013699 | [7] |
| $\mu_k$ | The bat death rate | 0.002747 | [7] |
| $\delta_m$ | Disease induced mortality rate in humans | 0.0436999 | [7] |
| $\delta_b$ | Disease induced mortality rate in pigs | 0.000374955 | [7] |
| $\delta_k$ | Disease induced mortality rate in bats | 0.000622043 | [7] |
| $\gamma_m$ | Recovery rate for humans | 0.0225626 | [7] |
| $\gamma_b$ | Recovery rate for pigs | 0.0692084 | [7] |
| $\gamma_k$ | Recovery rate for bats | 0.0750248 | [7] |
| $\theta_m$ | Immunity loss rate of recovered humans | 0.00153737 | [7] |
| $\theta_b$ | Immunity loss rate of recovered pigs | 0.000651486 | [7] |
| $\theta_k$ | Immunity loss rate of recovered bats | 0.000444376 | [7] |
| $\beta_m$ | Rates of transmission among humans | $1.39897 \times 10^{-8}$ | [7] |
| $\beta_b$ | Rates of transmission among pigs | $1.20377 \times 10^{-7}$ | [7] |
| $\beta_k$ | Rates of transmission among bats | 0.0000155344 | [7] |
| $\beta_{bm}$ | Pig to human transmission rate | $4.52495 \times 10^{-6}$ | [7] |
| $\beta_{km}$ | Bat to human transmission rate | $3.7756 \times 10^{-7}$ | [7] |
| $\beta_{kb}$ | Bat to pig transmission rate | $5 \times 10^{-6}$ | assumed |

Some of the figures below represent numerical simulations of the system's solutions. Figure 2 illustrates the temporal dynamics of the infectious human population ($I_m$) under two scenarios: with optimal control and without control intervention.

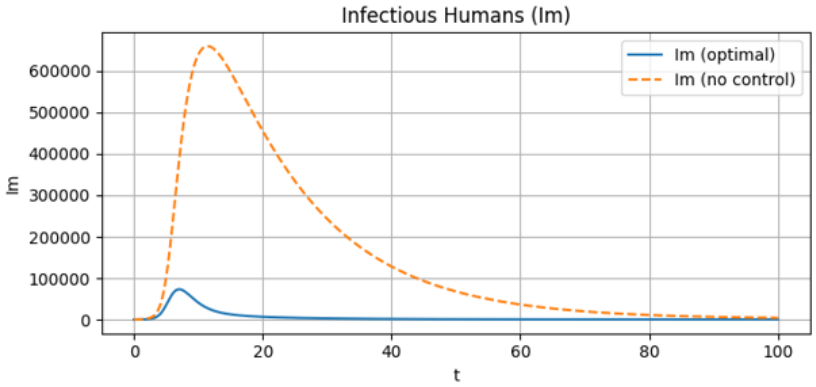


**Figure 2.** Dynamics of infectious humans ($I_m$) with and without optimal control.

Based on Figure 2, the infected human population under the control strategy is substantially reduced compared to the uncontrolled scenario. With control, the peak number of infectious individuals reaches approximately 70,000, whereas without control it exceeds 650,000 individuals. In addition, the decline of the infection curve occurs much more rapidly when the control measures are applied, indicating a faster suppression of the outbreak.

Furthermore, the figure 3 illustrates the behavior of the system under different configurations of the control variables. Each control combination produces a distinct trajectory of the infected human population, demonstrating the varying effectiveness of the individual and combined control strategies.

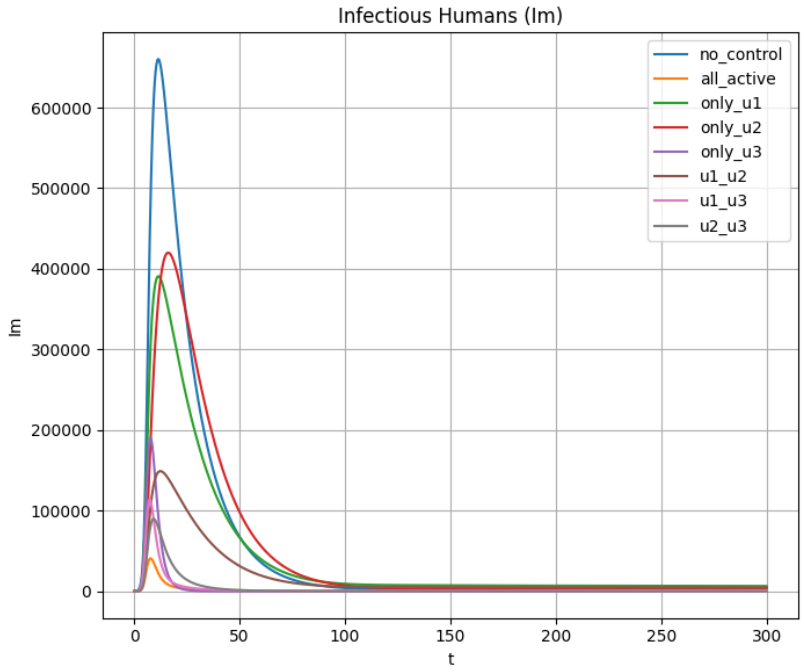


**Figure 3.** Infected human population under different control combinations

Figure 3 shows how different control combinations affect the number of infected humans. The uncontrolled scenario produces the highest peak, while activating all control variables yields the lowest and fastest-declining infection curve. Single controls ($u_1, u_2$, or $u_3$) reduce the peak to varying degrees, and combining two controls provides a stronger effect than using only one. Overall, the figure demonstrates that increasing the number and strength of control interventions leads to a more substantial reduction in infection levels.

Subsequently, the Figure 4 illustrates the dynamics of the infected pig population with and without the implementation of control measures. Under the control strategy, the peak number of infectious pigs is reduced to approximately 16,000 individuals, whereas in the absence of control, the peak exceeds 68,000 individuals. Moreover, the controlled trajectory declines much more rapidly, indicating a significantly faster suppression of infection within the pig population.

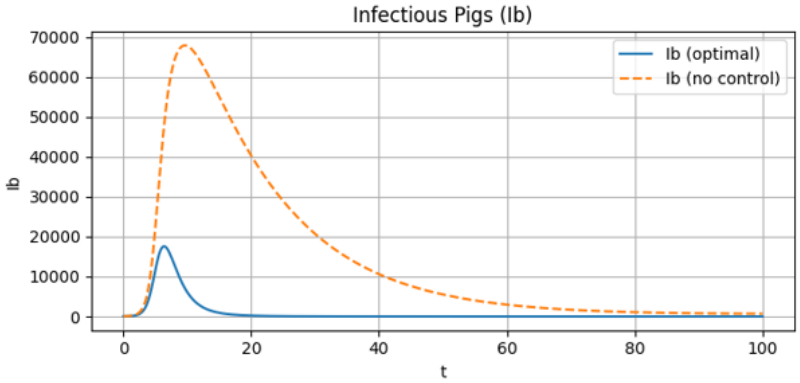


**Figure 4.** Dynamics of the infectious pig population ($I_b$) with and without optimal control intervention

Figure 5 presents the control profiles applied to the system. Based on Figure 5, $u_1(t)$ initially rises to its maximum level to rapidly suppress the infected pig population, and then gradually declines as the infection decreases. Meanwhile, $u_2(t)$ remains high during the early phase to minimize transmission, and slowly relaxes once the risk of infection becomes lower. This behavior reflects the optimal strategy of applying strong interventions when infection pressure is highest and reducing efforts as the system stabilizes.

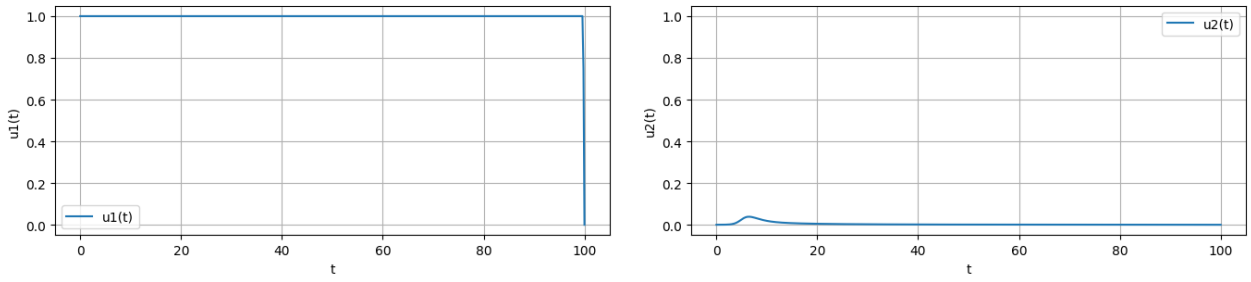


**Figure 5.** Control profiles $u_1(t)$ (culling of infected pigs) and $u_2(t)$ (preventive human animal protection measures)

Figure 6 shows time-dependent optimal control $u_3(t)$ for the isolation of infected humans. Likewise, $u_3(t)$ starts at a high level to immediately reduce human-to-human transmission. As the

number of infected individuals declines, the isolation effort gradually decreases, indicating that intensive isolation is most necessary during the peak transmission period and can be relaxed once the infection burden becomes lower.

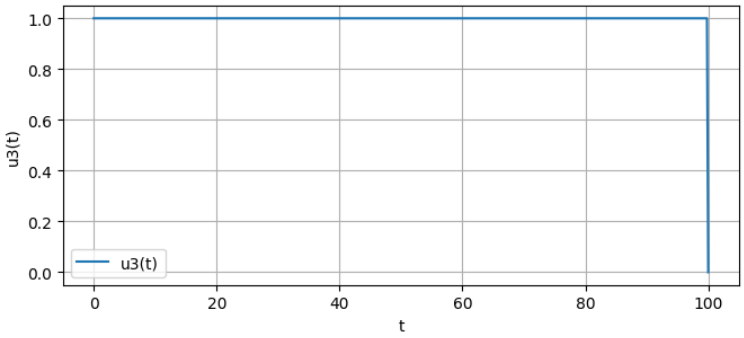


**Figure 6.** Time-dependent optimal control $u_3(t)$ for the isolation of infected humans.

## 4. DISCUSSION

The proposed multi-host SIRS model captures the transmission dynamics of Nipah virus among bats, pigs, and humans by incorporating reinfection mechanisms and heterogeneous interspecies contacts. The simulation results indicate that, without intervention, infection can spread rapidly through the pig population and subsequently generate substantial secondary transmission to humans. This reflects the important epidemiological role of pigs as an amplifying host, consistent with historical Nipah outbreaks in which close contact with infected pigs significantly increased human exposure. The marked reduction in both infected pigs and human cases under optimal control suggests that interrupting transmission at the animal–human interface is essential for outbreak containment.

The numerical results further demonstrate that each control strategy contributes differently to disease mitigation. The infected-pig culling strategy ($u_1$) directly reduces the reservoir of infectious pigs and therefore has a strong immediate effect on lowering onward transmission. Protective measures for human–animal contact ($u_2$) decrease exposure risk among susceptible humans and are particularly important in occupational settings such as farms or slaughterhouses. Human isolation efforts ($u_3$) help reduce secondary spread among humans once spillover infections occur. When implemented simultaneously, the three controls generate the fastest and most substantial decline in prevalence, indicating that integrated interventions are more effective than isolated single-control actions. This finding highlights the importance of combining veterinary and public health responses in zoonotic disease management.

These findings are broadly consistent with previous studies on Nipah virus and other zoonotic infections, which emphasize the critical role of animal reservoir management, movement restrictions, biosecurity practices, and early case isolation in preventing epidemic escalation. Several mathematical modeling studies have similarly reported that combined strategies outperform single interventions because they target multiple transmission pathways simultaneously. In particular, reducing infection in intermediate animal hosts has been recognized as one of the most efficient ways to prevent human outbreaks. This conclusion is in line with earlier NiV modeling studies that applied optimal control only to the human population through awareness, treatment, quarantine, or healthcare interventions

[13,15,18], where integrated controls were shown to reduce infection more effectively than single measures. It also complements previous models involving multiple host species, such as human–bat systems and three-species human–pig–bat frameworks [1,2,17], which highlighted the epidemiological importance of animal reservoirs and intermediate hosts in sustaining transmission. Compared with those studies, the present work extends the analysis by incorporating reinfection dynamics together with simultaneous controls targeting pigs, human exposure, and human isolation, thereby providing a more comprehensive multi-host intervention framework.Despite these useful insights, the present study has several limitations. First, parameter values were selected from available literature and assumed estimates, while comprehensive outbreak-specific data remain limited. Second, the model assumes homogeneous mixing within each host population, which may oversimplify real contact patterns. Third, environmental transmission, seasonal bat migration, farm heterogeneity, and demographic variability were not explicitly incorporated. Fourth, deterministic dynamics may underestimate the role of random effects during the early stage of outbreaks or in small populations.

Future research may extend the model in several directions. Incorporating real surveillance data would improve parameter estimation and predictive reliability. Stochastic formulations could better represent random outbreak fluctuations, while spatially explicit models may capture geographic spread between farms and communities. Network-based transmission structures could also reflect heterogeneous contact behavior. In addition, more advanced control frameworks, such as time-delay control, adaptive interventions, vaccination strategies, or cost-effectiveness optimization under limited resources, would provide valuable guidance for policymakers.

## 5. CONCLUSIONS

A multi-host SIRS model involving bats, pigs, and humans was constructed to represent the interspecies transmission patterns of Nipah virus, incorporating reinfection and heterogeneous contact routes. Three time-dependent controls infected pig culling ($u_1$), human animal protective measures ($u_2$), and human isolation efforts ($u_3$) were introduced to assess effective intervention strategies. Using optimal control theory, the existence of an optimal control set was verified, and Pontryagin's Maximum Principle provided explicit expressions for the optimal controls. Numerical simulations showed a substantial reduction in infections: peak human cases declined from over 650,000 to about 70,000, and peak infected pigs dropped from more than 68,000 to roughly 16,000 under optimal control. The control profiles reveal that strong early interventions across all three measures are crucial for rapid suppression, followed by a gradual decrease in effort as infections diminish. Overall, combining all controls yields the fastest and most pronounced reduction in disease prevalence, highlighting the importance of coordinated, multi-component strategies to effectively mitigate Nipah virus transmission across species.

## ACKNOWLEDGEMENTS

The author would like to thank the Faculty of Mathematics and Natural Sciences, Universitas Bengkulu, for the support provided to complete this research. This work was funded through the FMIPA RBA scheme under the *Pembinaan* research program, Contract No. 4554/UN30.12/HK/2025.

## REFERENCES


[1] A. D. Zewdie, S. Gakkhar, and S. K. Gupta, "Human–animal Nipah virus transmission: model analysis and optimal control," *Int. J. Dyn. Control*, vol. 11, no. 4, pp. 1974–1994, 2023, doi: 10.1007/s40435-022-01089-y.

[2] M. Xie, M. Y. Khan, S. Ullah, M. Farooq, M. B. Riaz, and B. Al Alwan, "Optimal control analysis for the transmission of Nipah infection with imperfect vaccination," *PLoS One*, vol. 20, no. 4 April, pp. 1–26, 2025, doi: 10.1371/journal.pone.0317408.

[3] Vijay K. Chattu, Raman Kumar, Soosanna Kumary, Fnu Kajal, and Joseph K. David, "Nipah virus epidemic in southern India and emphasizing'One Health' approach to ensure global health security," *J. Fam. Med. Prim. Care*, vol. 7, no. 2, pp. 275–283, 2018.

[4] K. Halpin *et al.*, "Pteropid bats are confirmed as the reservoir hosts of henipaviruses: A comprehensive experimental study of virus transmission," *Am. J. Trop. Med. Hyg.*, vol. 85, no. 5, pp. 946–951, 2011, doi: 10.4269/ajtmh.2011.10-0567.

[5] H. Li, J. Y. V. Kim, and B. S. Pickering, "Henipavirus zoonosis: outbreaks, animal hosts and potential new emergence," *Front. Microbiol.*, vol. 14, no. July, 2023, doi: 10.3389/fmicb.2023.1167085.

[6] D. J. Middleton *et al.*, "Experimental Nipah virus infection in pigs and cats," *J. Comp. Pathol.*, vol. 126, no. 2–3, pp. 124–136, 2002, doi: 10.1053/jcpa.2001.0532.

[7] S. Barua and A. Dénes, "Global dynamics of a compartmental model for the spread of Nipah virus," *Heliyon*, vol. 9, no. 9, p. e19682, 2023, doi: 10.1016/j.heliyon.2023.e19682.

[8] K. B. Chua, "Nipah virus: A recently emergent deadly paramyxovirus," *Science (80-. ).*, vol. 288, no. 5470, pp. 1432–1435, 2000, doi: 10.1126/science.288.5470.1432.

[9] K. B. Chua, "Nipah virus outbreak in Malaysia," *J. Clin. Virol.*, vol. 26, no. 3, pp. 265–275, 2003, doi: 10.1016/S1386-6532(02)00268-8.

[10] P. D. Yadav *et al.*, "Nipah Virus Outbreak in Kerala State, India Amidst of COVID-19 Pandemic," *Front. Public Heal.*, vol. 10, no. February, 2022, doi: 10.3389/fpubh.2022.818545.

[11] M. Arulmohi, V. Vinayagamoorthy, and D. A. R., "Physical Violence Against Doctors: A Content Analysis from Online Indian Newspapers," *Indian J. Community Med.*, vol. 42, no. 1, pp. 147–50, 2017, doi: 10.4103/ijcm.IJCM.

[12] E. Rahardianingtyas *et al.*, "Nipah Virus Detection in Pteropus hypomelanus Bats, Central Java, Indonesia," vol. 31, no. 4, pp. 867–870, 2025.

[13] E. N. R. Ilmayasinta, N., Soemarsono, A. R., Aishwaray, "Model Matematika Penyebaran Virus Nipah (NiV) dengan Kontrol Optimal menggunakan Metode Pontryagin Maximum Principle (PMP)," vol. 14, no. 1, pp. 95–108, 2022.

[14] M. K. Mondal, M. Hanif, and M. H. A. Biswas, "A mathematical analysis for controlling the spread of Nipah virus infection," *Int. J. Model. Simul.*, vol. 37, no. 3, pp. 185–197, 2017, doi: 10.1080/02286203.2017.1320820.

[15] J. Sultana and C. N. Podder, "Mathematical Analysis of Nipah Virus Infections Using Optimal Control Theory," *J. Appl. Math. Phys.*, vol. 4, no. 5, pp. 1099–1111, 2016, doi: 10.9734/air/2016/30992.

[16] D. Baleanu, P. Shekari, L. Torkzadeh, H. Ranjbar, A. Jajarmi, and K. Nouri, "Stability analysis and system properties of Nipah virus transmission: A fractional calculus case study," *Chaos, Solitons and Fractals*, vol. 166, no. November 2022, p. 112990, 2023, doi: 10.1016/j.chaos.2022.112990.

[17] S. Barua, M. A. Ibrahim, and A. Dénes, "A compartmental model for the spread of Nipah virus in a periodic environment," *AIMS Math.*, vol. 8, no. 12, pp. 29604–29627, 2023, doi: 10.3934/math.20231516.

[18] S. Rosnafi'an Sumardi, C. Bintang, G. Allo, W. Ade Fitriya B, and N. R. Paranoan, "DENGAN MENGGUNAKAN KENDALI OPTIMAL METODE Pontryagin Maximum Principle (PMP)," *J. Multidisiplin Ilmu*, vol. 2, no. 1, pp. 2828–6863, 2023.

[19] F. Evirgen, "Transmission of Nipah virus dynamics under Caputo fractional derivative," *J. Comput. Appl. Math.*, vol. 418, no. April 2001, p. 114654, 2023, doi: 10.1016/j.cam.2022.114654.

[20] A. Malek, N. Islam, and A. Hoque, "Informatics in Medicine Unlocked Investigations of transmission dynamics of Nipah virus in Bangladesh," *Informatics Med. Unlocked*, vol. 44, no. November 2023, p. 101417, 2024, doi: 10.1016/j.imu.2023.101417.

[21] J. Khalil, Z H., Rimi., M., Mouline, "Modeling nipah virus dynamics and designing optimal control strategies," *Commun. Math. Biol. Neurosci*, vol. 45, no. 1, pp. 1–26, 2025.

[22] J. A. Bather, W. H. Fleming, and R. W. Rishel, *Deterministic and Stochastic Optimal Control.*, vol. 139, no. 4. 1976. doi: 10.2307/2344363.